An Electrodeposition Process Followed by X-ray Microscopy

S. Rondot,*,† O. Aaboubi,‡ J. Cazaux,† and A. Olivier‡

LASSI/LECS DTI EP120 CNRS, Faculté des Sciences, B.P. 1039, 51687 Reims Cedex 2, France

Received: January 13, 1997; In Final Form: June 17, 1997[⊗]

Time-dependent X-ray microscopy has been applied for the first time to follow an electrodeposition process: that of copper on a glassy carbon electrode. From a series of X-ray microradiographs taken every 20 s it is possible not only to measure directly the increasing thickness of the coating but also to evaluate the copper sulfate concentration profile in the electrolyte at the corresponding instants of acquisition. When the electrodeposition conditions lead to ramified growth close to coating/electrolyte interface, local variations of the ionic concentration are observed as a function of time and of coordinates. The lateral resolution is in the 10−20 μm range and relative concentration changes of few percent are easily detected.

1. Introduction

Electrochemical deposition (ECD) has attracted much attention for a long time and the role of the various parameters such as salt formula, cell geometry, concentration of the solution, applied potential, etc., on the growing process has been extensively explored.[1−5] The experimental investigations are mainly based on the classical three-electrode arrangement which is followed by the examination of the deposit. This approach requires the experiment to be stopped so that it is time consuming and its microscopic results are hardly connected with the solutions of Fick's equations. More generally in electrochemistry there are on the one hand a proliferation of microscopic models which try to describe what may happen in the electrolyte and on the other hand a proliferation of experimental results on the deposit but rather few experimental methods are able to give local information (such as ionic concentrations at the micrometer scale) in the electrolyte and change as a function of time and operating conditions.

In order to visualize the fluid motion, the use of interference contrast optical microscopy seems to be presently one of the most efficient techniques despite the facts that it often requires the use of tracers such as oil droplets and that the principle of the method only gives the difference in the refractive index experienced by two optical beams. Afterwards, this difference requires to be related to the corresponding concentration change.[6,7]

Previously, the implementation of spectroelectrochemistry based on the measurement of the absorbance, by the dilute species, of a monochromatic light diffracted by the working electrode, allowed determination of the local concentration of the absorbing species in the diffusion layer close to the electrode.[8] But despite the very good detection limit of this technique around 10^{-8} M, concentration is measured only in specific conditions for which the absorbance of light by the species is linearly related to concentration in the Beer's law fashion. Moreover, the technique requires a colored main species and a colorless environment for this species.

We believe that X-ray microscopy offers an alternative experimental solution for the direct investigation of ions moving in solution as it has been showed for the direct observation of zinc ions diffusing in aqueous hydrochloric acid solution during the corrosion process of zinc foils and pellets.[9] Indeed it allows to obtain the concentration maps of the colorless species from a whole image of the process acquired with a lateral resolution similar to those obtained with the laser-based technique.

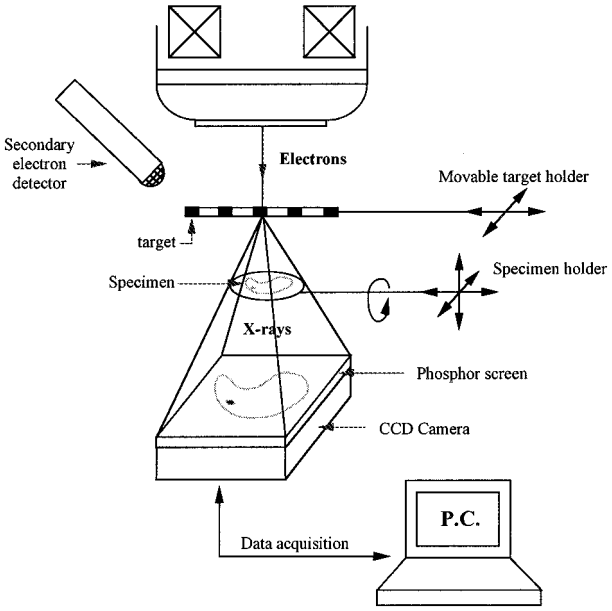

Figure 1. Sketch and description of the X-ray microscope.

The goal of the present paper is to report on the first application of this technique to study an electrodeposition process (copper on a glassy carbon electrode) with the periodic acquisition of X-ray microradiographs every 20 s having a lateral resolution in the 10−20 μm range. The experimental arrangement is described in the next section. The experimental results obtained in two different regimes are developed in section 3.

2. Experimental Arrangement

2.1. The X-ray Microscope Used in the Experiments. We used an X-ray projection microscope derived from a conventional scanning electron microscope equipped with a cooled CCD camera.[10−12] Its principle is illustrated in Figure 1. The incident electron beam (of energy in the 10−30 keV range) generates a conical X-ray illumination on the specimen from the bombardment of a thin foil target (a few micrometers thick).

* Corresponding author. E-mail: sebastien.rondot@univ-reims.fr. Fax : (33) 326 053312.
† LASSI
‡ LECS.
⊗ Abstract published in *Advance ACS Abstracts,* August 1, 1997.

S1089-5647(97)00389-1 CCC: $14.00

The geometrically magnified X-ray image is transformed into visible image by the use of a phosphor converter and this last image is collected by a Peltier-cooled CCD camera via a fiber optic bundle set between the phosphor converter and the CCD itself. Different targets placed side by side on a movable target holder permit variation of the energy of the incoming photons without any intervention in the vacuum chamber. The choice of the nature of the target allows the optimization of the sensitivity of the technique for the detection of the element of interest. When medium elements are embedded in very light matrices such as water, the detection limit may reach 10 ppm (10^{-5} at./at.).[15] In the present experiment, a Zr target 3 μm thick has been used for improving the detection of Cu ions in solution : the absorption edge of Cu is situated at $E_{\mathrm{Cu(K\ edge)}} \approx$ 9 keV while the characteristic photon energy issued from the target is $E(\mathrm{Zr\ K}\alpha) = 15.8$ keV.

The lateral resolution of the microscope is governed by geometrical considerations depending upon the exact position of the specimen between the X-ray source and the detector. It ranges from the size of the X-ray source ($s \approx 1\ \mu$m) to the size ($D \approx 22\ \mu$m) of an element detector of the CCD camera.[10−12] In the present experiment, the specimen being situated at half the distance between the source and the detector, the lateral resolution is in the order of 10 μm.

Digitalized projection images (385 × 578 pixels) are generally acquired in a few seconds and these images can be processed next for quantitative imaging: Three successive images are obtained: the first, B, without either the specimen or the illumination (to obtain the dark noise of the CCD alone); the second one, E, with the X-ray beam but not the specimen (to obtain, for each pixel, the incident photon beam intensity); and the third one, I, with the incident X-rays and the specimen (microradiograph of the object). Taking next, pixel by pixel, the logarithm of the ratio (E − B)/(I − B), a μt map of the specimen is then obtained for the characteristic radiation E generated by the thin foil target.

The advantages of the CCD detector are its speed, its good linearity, and its wide dynamic range (ratio of saturation signal to readout noise up to 3×10^4). These advantages lead, here, to rapid image acquisition (a few seconds) and to a time series of images tens of seconds distant from each other.

Because of the nature of our X-ray microscope, the specimen is placed into the vacuum chamber. Study of time-dependent chemical reaction in a liquid required the design of an environmental chamber (hermetic solution cell), which holds the specimen in solution at atmospheric pressure. Our cell made of polyacrylic has two silicon pipes which connect the outside of the microscope to its vacuum chamber by means of a feedthrough. This permits one to set the copper sulfate solution inside the cell and to measure outside the reference potential of the electrochemical system (Figure 2). Two removable face to face PTFE screws permit to place a glassy carbon and a copper electrode. Basically, this cell is derived from those used to follow zinc ions diffusion in solution.[9] The position of the cell in the X-ray microscope can be seen in Figure 3.

2.2. The Electrochemical Procedure. The electrochemical reaction is a classic one where a copper electrode is oxidized and incoming copper ions are coated on a glassy carbon electrode. It uses three electrodes: a working electrode (glassy carbon), a counter electrode (copper), and a reference electrode (saturate sulfate electrode: SSE). Each of the two polarized electrodes (carbon and copper) are cylinders 3 mm in diameter. Therefore, the polished surface of each electrode is a disc. The electrolyte is a 0.2 mol·L^{-1} copper sulfate solution added with a 0.5 mol·L^{-1} sulfuric acid solution. The acid ensures the electric current flow in the solution. The reference electrode is set outside in a container filled with the copper sulfate solution in which one of the capillaries (connecting the cell to the outside) filled with the same solution is immersed. This setup permits measurement of reference potential and avoids the conception of a complicated three-electrode hermetic cell.

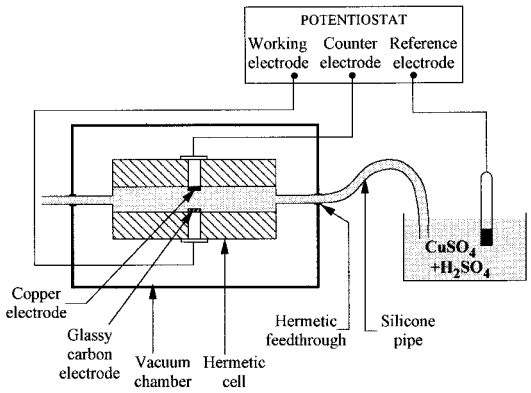

Figure 2. Sketch of the hermetic cell with the electrochemical procedure.

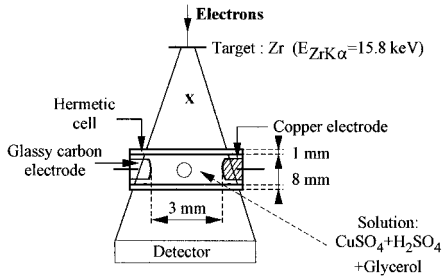

Figure 3. Observation geometry of the electrochemical process in the cell.

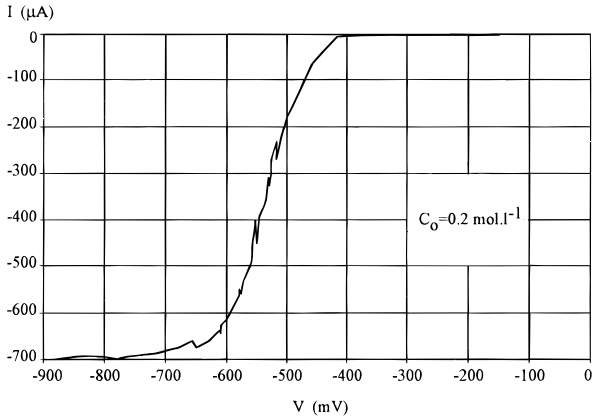

Figure 4. Intensity vs potential curves during the experiment 3.2. From this curve it is easy to see that the constant potential to choose is between −700 and −550 mV.

In the electrochemical conditions of experiment 3.2, $E = -575$ mV/SSE, the copper deposition on carbon is mainly driven by the copper ions diffusion process at the electrode/solution interface.

The polarization is controlled by a potentiostat which allows measurement of the carbon electrode potential in comparison with the reference electrode potential. Figure 4 shows the experimental intensity vs potential curve acquired during experiment 3.2. It gives a survey of the evolution of the current and permits to choose the value of the overpotential. From this graph, it seems that the appropriate potentiostatic polarization is between −700 and −550 mV.

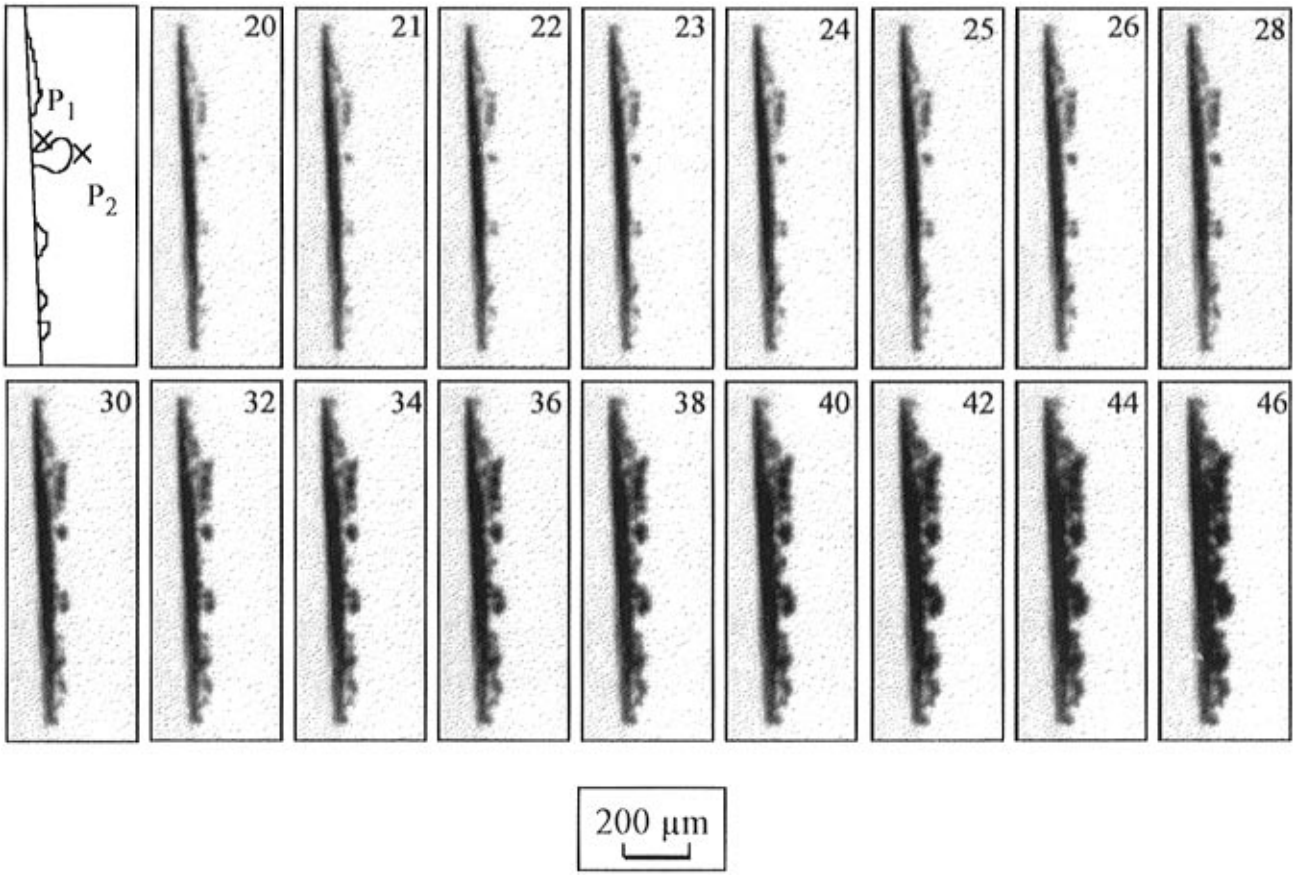

Figure 5. (Top left) Representation of the two measurement points for curves of Figure 6. Time series of images showing the evolution of the ramified growth in black of the deposit in experiment 3.1. Number on the top right of each image indicates time in minutes.

3. Experimental Results

Two series of electrochemical experiments were performed. In the first series, the electrochemical condition was $E = -0.760$ V/ESS. In the second series, the condition was less stringent: $E = -0.575$ V/ESS. For these two in situ copper electrodeposition experiments, the same procedure for the data acquisition and image processing has been used. Besides the periodic image acquisitions during the process, they both consist, first, in the acquisition of two images: that of the empty cell and that of the cell filled with the solution when no polarization is applied between the electrodes. From the well-known Beer's law describing the attenuation of monochromatic X-rays: $I = I_0 e^{-\mu t}$ (with I, I_0 transmitted and incident intensities, and μ, t linear absorption coefficient and thickness of the specimen, respectively) it is convenient to submit every pixel of each image to a logarithmic compression ($i = \log(I_0/I)$) in order to subtract next the contribution of the empty cell. For the investigation of the ionic concentration change in the solution, this procedure leads to the local μt values for the liquid at each instant of acquisition and the same value $(\mu t)_0$ for the reference solution only. Consequently, by dividing next each local μt value by the corresponding value $(\mu t)_0$, one obtains the local relative concentration change of Cu^{2+} with respect to the standard concentration composed of 0.5 mol·L^{-1} $CuSO_4$ and 0.5 mol·L^{-1} H_2SO_4 . The remaining fraction is composed of water to which glycerol has been added in order to slightly slow down the diffusion process and to avoid convection process on the cell walls.

3.1. First Series of Electrochemical Experiments ($E = -0.760$ V/ESS). When stringent conditions are applied, the electrodeposition is not uniform and ramified deposition mechanism takes place.[6,7] The corresponding concentration profiles

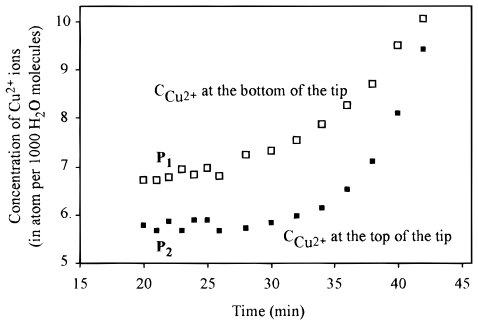

Figure 6. Comparison of the evolution of the concentration of the copper ions at the top and at the bottom of a tip for points P1 and P2.

are expected to change from place to place along the deposit/electrolyte interface. In such a situation, the advantage of X-ray microscopy seems obvious. This advantage is illustrated in Figure 5 in which the dendritic shape of the coating and its evolution as a function of time are shown. The image area, here, is restricted to the closest part of the electrode/solution interface. This area is not wide enough to allow measurement of the diffusion layer thickness. The main goal was the measurement of the concentration change close to the tips of the ramified deposit.

Selecting two points P1 and P2 in the solution where point P1 is taken at the bottom of a tip and P2 is taken at the top of the same tip (see insert of Figure 5), it is easy to obtain the experimental concentration change at these two points as a function of time. The corresponding curves are displayed on Figure 6. The two curves present a similar behavior with the increase in the local concentrations when the electrodeposition time is increased. They seem to reach the same final value: at $t = 45$ min, the final concentrations are nearly 50%−70% larger

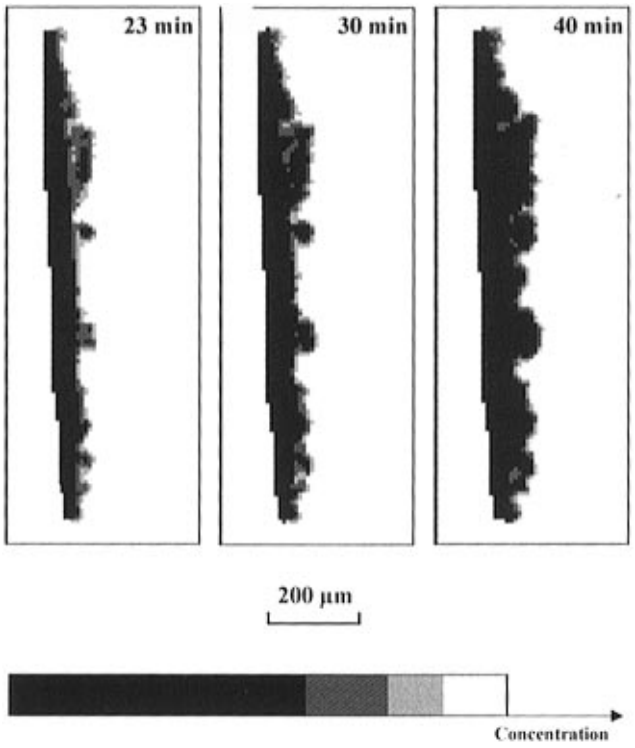

Figure 7. Contours (in light gray and dark gray) in a specific concentration range for three images of the dendritic coating of experiment 3.1. From the color scale, it is possible to see the local concentration gradients of copper ions close to the deposit.

than the initial ones. But it is also clear that the initial values differ from each other, the local concentration at the bottom being 15% larger than that at the top of the tip. Qualitatively, this result is explained by the fact that the local electric field on the top of the tip is larger than that on the bottom of the tip and the velocity of the ions varies in the same proportion, leading to the reverse behavior for the local ionic concentrations (when electrical current density is postulated to be a constant).

Instead of looking at the local concentration change as a function of time it is also possible to point out the copper concentration gradient in the liquid close to the deposit at a given instant. Figure 7 shows, for three different instants of the process and using a color table with four gray levels (black, dark gray, light gray, and white), two contours in light gray and dark gray each corresponding to a given concentration interval (see the colors scale on the same figure). Despite the lateral resolution used, they permit to see the copper concentration evolution close to the deposit. In specific places close to the top of a deposit tip, the colors change from white (on the right side) to dark gray without going through light gray showing an abrupt local copper concentration change in the liquid.

These changes could be better pointed out when working with a lower lateral resolution which could be achieved only by mean of a thinner hermetic cell (in order to reach a higher magnification in the microscope) and a smaller X-ray source size. We will proceed in the near future in this way with a more accurate in-situ study of a ramified coating of zinc in order to measure change in the diffusion layer thickness and the associated concentration variation between the middle of the solution and the deposit.

3.2. Second Series of Electrochemical Experiments ($E = -0.575$ V/ESS). The inset of Figure 8 gives view of the specimen geometry and the main part represents some selected images of the corresponding series. The image processing consists in the ratio of the difference between each image and the image of the empty cell with the difference between the image of the cell filled with the solution before any polarization and the image of the empty cell. The white area on the left part of each image represents the strong X-ray absorption of the copper coating on the glassy carbon electrode (left). More interesting are the central parts of each microradiograph presented in Figure 8. After the image processing indicated above, these central parts represent the change as a function of time and $x-y$ coordinates of the normalized concentration of the copper ions in the solution. Because the two electrodes are nearly parallel to each other and to the y direction, it is possible to draw the mean concentration profile along the x direction by averaging the information contained in each raw (parallel to y). These mean concentration profiles are represented on the bottom of each image. From these profiles, it is clear that the concentration change is nearly a plateau in the region localized between the electrodes and the distances larger than saying 200 μm from the corresponding interfaces. From one image to another, the height of this plateau fluctuates from 1.115 up to 1.130 with respect to the concentration of the standard. This fluctuation may be due to electron beam intensity fluctuations (and then to the erratic change of incident X-ray intensity during the process). The fact that the concentrations corresponding to each plateau are more than 10% larger than that of the standard solution (without polarization) can be explained by a sudden change in the incident electron beam intensity between the measurement of the standard solution and the acquisition of the successive projection images.

Finally, there is the selective concentration change that can be clearly identified on each profile close to the glassy carbon electrode. This decrease is independent of the possible artifacts mentioned above and it corresponds qualitatively to the expected change in the diffusion layer.

Quantitatively from the enlarged profile as that shown in Figure 9, it can be seen that the measured mean thickness d of this layer is around 239 ± 30 μm and the relative change in concentration ΔC is $(1.74 \pm 0.17) \times 10^{-3}$ mol·L^{-1}. From the profile, it can be seen that the determination of the thickness of the diffusion layer is not obvious because of the need to approximate the limit of the concentration change. More, the ΔC value is very low and shows that the concentration of the ions on the electrodes is not necessarily nil in this kind of diffusion-controlled electrodeposition process.

This experimental result is in good agreement with the following theoretical considerations. When the current I reaches the cathodic limit value $I = 0.7$ mA, its expression, derived from the first Fick's law, is the following one:

$$I = zFAD(C_0/\delta) \tag{3.1}$$

This equation corresponds to the Nernst model in which z is the number of charges of the deposited species (Cu^{2+}), F is the charge of a mole of electrons, A is the surface of the carbon electrode, D is the mean diffusion coefficient of Cu^{2+} ions, C_0 is the initial concentration of the copper sulfate solution (0.2 mol·L^{-1}), and δ is the thickness of the diffusion layer.

Chronopotentiometric measured values of D for $CuSO_4$ at 25 °C can be found in Quickenden and Jiang's paper.[14] In our case, $D \approx 7 \times 10^{-6}$ cm^2·s^{-1}.

On the one hand, the calculation using eq 3.1 leads to $\delta = 270$ μm for the diffusion layer which is close to the experimental value measured by X-ray microscopy ($\delta = 239$ μm). This gives evidence that X-ray microscopy is a method well suited for measurement of the thickness of the diffusion layer in this kind of electrodeposition process. On the other hand, using eq 3.1, we do not find a correlation between experimental value for

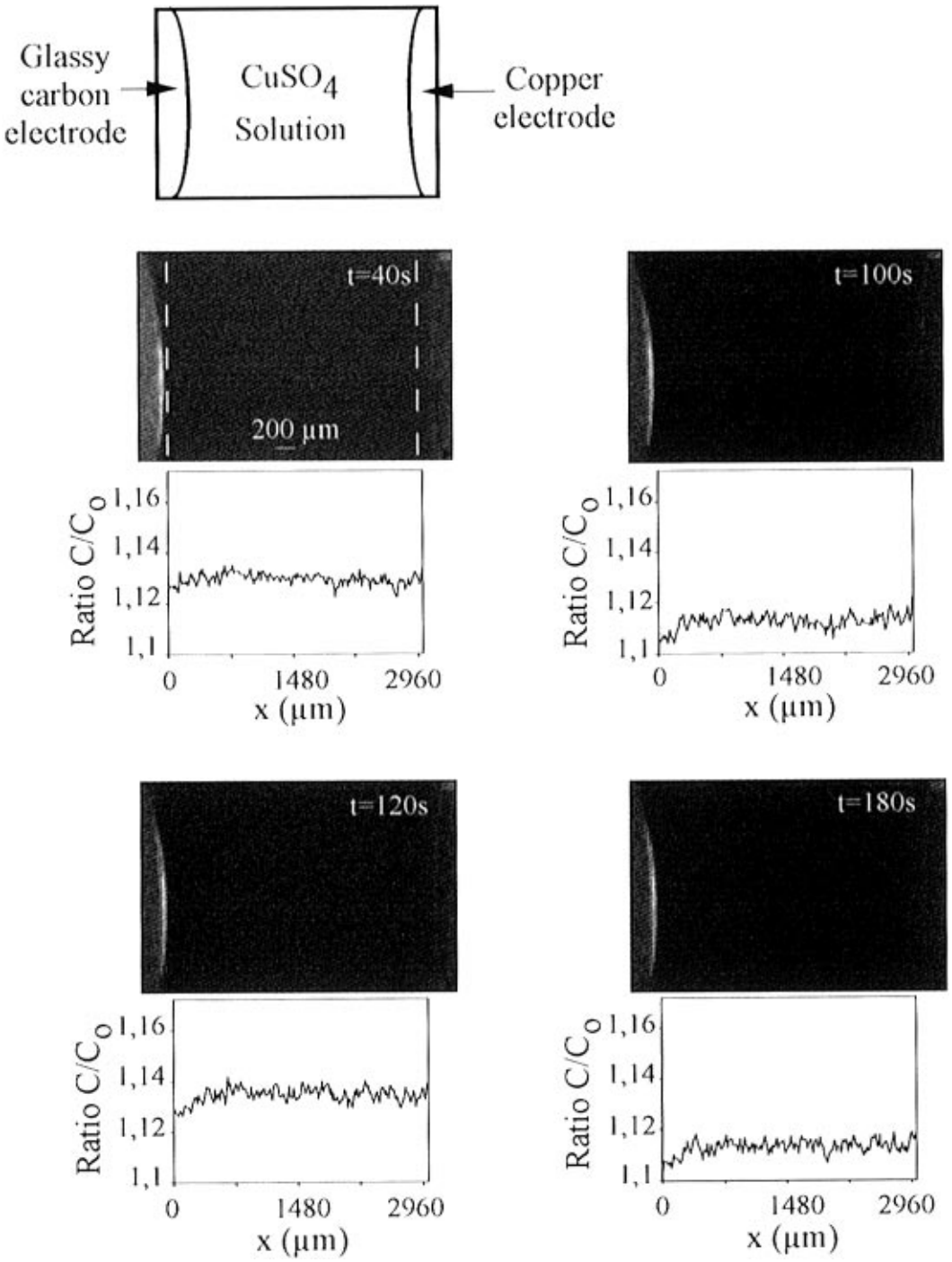

Figure 8. (top left) Sketch of the electrochemical system. Images of the electrodes and the solution at four instants with the corresponding average profiles along the *x* direction, each showing the decrease of the concentration of the copper ions close to the electrode.

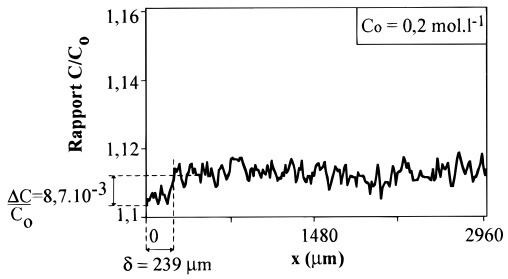

Figure 9. Measurement of the thickness δ of the diffusion layer and of the concentration change ΔC at the electrode/solution interface for the given profile of the image acquired at $t = 100$ s.

ΔC and the value deduced from the model. This could partly be explained in the following way: because we work with projection images of the specimen, the measurements give mean values of the concentration change in the *z* direction. More, as the electrode is a disc, the concentration gradients on the center and on the border are not the same, so the average profile may lead to a measured concentration change value lower than the real one. As this concentration change in the liquid, close to the working electrode, is very low and as the thickness of the diffusion layer is not easy to determine, their evaluation by X-ray microscopy is an interesting challenge.

4. Conclusion

Owing to the ability to follow in situ the evolution of the ions concentrations in an electrodeposition process by X-ray microscopy it is possible to detect the end of the diffusion layer

and the concentration change in a diffusion-controlled process. More, the local concentration gradient in the liquid, close to the deposit tip of a ramified coating, can be deduced. An improvement of our experiment would be a lower lateral resolution in order to see more accurately what happens at the electrode/solution interface. But, for this purpose, it is necessary to build a thinner hermetic cell.

When compared to other investigation methods, X-ray microscopy allows analysis of the electrochemical reaction, as a function of time, without bringing any change to the process evolution and with a wide depth of field. The lateral resolution of our technique around 20 μm is good enough to investigate concentration variation in the diffusion layer and a nanometer resolution method such as near field microscopy would be unable to analyze and quantify perturbed environment, close to the tips of a ramified deposit, as that presented on Figure 7.

This sort of analysis should lead to a better understanding of the concentration changes at the electrode/solution interface in mass transport controlled electrochemical processes, this mass transport being generated by temperature change, potential difference, or composition change.

In order to go further, it is possible to analyze chemical or electrochemical processes involving more than one metallic species with the determination of the concentration change of each species for each recorded moment of the process.[15]

In the near future we plan to study electrochemical processes disturbed by a local thermal or magnetic excitation which are part of the research work of two of us.

References and Notes

(1) Gorbunova, K. M.; Tkachik, Z. A. *Electrochim. Acta* **1971**, *16*, 191.
(2) Ibl, N.; Schadegg, K. *J. Electrochem. Soc.* **1967**, *114*, 54.
(3) Ogata, Y.; Yamakawa, K.; Yoshizawa S. *J. Appl. Electrochem.* **1983**, *13*, 611.
(4) Fukunaka, Y.; Doi, H.; Kondo, Y. *J. Electrochem. Soc.* **1990**, *137*, 88.
(5) Popov, K. I.; Pavlovic, M. G.; Macsimovic, M. D. *J. Appl. Electrochem.* **1982**, *12*, 525.
(6) Fleury, V.; Chazalviel, J. N.; Rosso, M. *Phys. Rev. E* **1993**, *48*, 1279.
(7) Fleury, V.; Kaufman, J. H.; Hibbert, D. B. *Nature* **1994**, *367*, 435.
(8) Jan, C. C.; Lavine, B. K.; McCreery, R. L. *Anal. Chem.* **1985**, *57*, 752.
(9) Rondot, S.; Cazaux, J.; Aaboubi, O.; Chopart, J. P.; Olivier, A. *Science* **1994**, *263*, 1739.
(10) Thomas, X.; Cazaux, J.; Erre, D.; Mouze, D.; Collard, P. In *X-ray Microscopy III*; Michette, A. G., Morrisson, G. R., Buckley, C. J., Eds.; Springer Series in Opt. Sci.; Springer Verlag: Berlin, 1992; Vol. 67, 190.
(11) Cazaux, J.; Elhila, H.; Erre, D.; Mouze, D.; Patat, J. M.; Rondot, S.; Trebbia, P.; Zolfaghari, A. *Microsc. Anal.* **1994**, *29*, 19.
(12) Cazaux, J.; Erre, D.; Mouze, D. Patat, J. M. Rondot, S. Sasov, A. Y. Trebbia, P. Zolfaghari, A. *J. Phys. IV, Colloque G7* **1993**, 2099.
(13) Cazaux, J. *Microsc. Microanal., Microstruct.* **1993**, *4*, 513.
(14) Quickenden, T. I.; Jiang, X. *Electrochim. Acta* **1984**, *29 (6)*, 693.
(15) Rondot, S.; Cazaux, J. *Ultramicroscopy* **1996**, *65 (3−4)*, 159.